BIOCHEMISTRY
including biophysical chemistry & molecular biology
Article

Biochemistry **2009,** *48,* 9941–9948 9941
DOI: 10.1021/bi901425h

Transition State Analogues Rescue Ribosomes from Saporin-L1 Ribosome Inactivating Protein†

Matthew B. Sturm,‡ Peter C. Tyler,§ Gary B. Evans,§ and Vern L. Schramm*,‡

‡*Department of Biochemistry, Albert Einstein College of Medicine, Bronx, New York 10461, and* §*Carbohydrate Chemistry Group, Industrial Research Ltd., Lower Hutt, New Zealand*

Received August 14, 2009; Revised Manuscript Received September 16, 2009

ABSTRACT: Ribosome inactivating proteins (RIPs) catalyze the hydrolytic depurination of one or more adenosine residues from eukaryotic ribosomes. Depurination of the ribosomal sarcin−ricin tetraloop (GAGA) causes inhibition of protein synthesis and cellular death. We characterized the catalytic properties of saporin-L1 from *Saponaria officinalis* (soapwort) leaves, and it demonstrated robust activity against defined nucleic acid substrates and mammalian ribosomes. Transition state analogue mimics of small oligonucleotide substrates of saporin-L1 are powerful, slow-onset inhibitors when adenosine is replaced with the transition state mimic 9-deazaadenine-9-methylene-*N*-hydroxypyrrolidine (DADMeA). Linear, cyclic, and stem−loop oligonucleotide inhibitors containing DADMeA and based on the GAGA sarcin−ricin tetraloop gave slow-onset tight-binding inhibition constants (K_i*) of 2.3−8.7 nM under physiological conditions and bind up to 40000-fold tighter than RNA substrates. Saporin-L1 inhibition of rabbit reticulocyte translation was protected by these inhibitors. Transition state analogues of saporin-L1 have potential in cancer therapy that employs saporin-L1-linked immunotoxins.

Ribosome inactivating proteins (RIPs) are *N*-glycohydrolases that catalyze the depurination of adenosine A_{4234} from the highly conserved sarcin−ricin loop of the 28S eukaryotic ribosomal subunit RNA (*1*). Depurination inhibits the binding of elongation factor 2 to the ribosome, halts protein synthesis, and causes cell death (*2*). RIPs with broad polynucleotide:adenosine glycosidase activity can target other ribosomal sites and nonribosomal substrates, including DNA, RNA, and poly(A) (*3*, *4*). Saporin-L1 toxin, a RIP from the leaves of the *Saponaria officinalis* plant, can release adenine from poly(A), herring sperm DNA, tRNA, *Escherichia coli* rRNA, and globin mRNA at physiological pH (*5*, *6*). Fifteen saporin isoforms have been characterized from *S. officinalis*, including nine seed, three leaf, and three root RIPs. These isoforms differ in ribosome translation inhibition activity and nascent cellular toxicity (*7*). Analysis of 50 type I and II RIPs revealed only saporin-L1 with the ability to release adenine from RNA of MS2, TMV, and AMCV viruses at physiological pH, a catalytic activity unique in the RIP family of enzymes (*3*).

Our goal is to develop transition state analogue inhibitors of ribosome inactivating proteins. These may find use in rescue therapy, by preventing the vascular leak syndrome sequelae common in clinical trials of RIPs linked to antibodies directed against cancer epitopes. Such inhibitors could provide extracellular protection against circulating toxins. We model these inhibitors on the transition state of ricin A-chain, the only RIP for which transition state information is available. Kinetic isotope effect studies established that ricin A-chain hydrolysis of 10-mer RNA and DNA stem−loop substrates occurs through leaving group activation and forms ribooxacarbenium ion transition states (*8*−*10*). Small RNA stem−loop structures are substrates for RIPs, and stem−loop substrate mimics of the sarcin−ricin loop serve as inhibitor scaffolds. Substrate stem−loop structures contain a GAGA tetraloop for RIP recognition and alternating C-G base pairs for stem stability and loop folding (Figure 1). Transition state analogues for ricin A-chain featured protonated 1-aza sugars to mimic the oxacarbenium ion intermediate and leaving groups with an elevated pK_a at the depurination site (*8*). Ricin A-chain shows robust catalytic activity on stem−loop RNA substrates at pH 4 but is inactive with these substrates at neutral pH. Transition state analogues of ricin A-chain are nanomolar inhibitors at pH 4 but did not protect ribosomes from ricin A-chain action at neutral pH. Therefore, we searched for another RIP with robust catalytic activity at physiological pH values and with the ability to be inhibited by transition state analogues, a prelude to use as an anticancer agent when linked to an appropriate recognition motif (*11*). Powerful inhibitors of the toxin can then provide an extracellular, circulating rescue agent to prevent the post-therapy vascular leak syndrome commonly associated with RIP immunochemotherapy (*12*).

Saporin-L1 has not been kinetically characterized with small substrates or inhibitors. Here we characterize its kinetic properties on small stem−loop substrates and on mammalian ribosomes and report novel transition state analogue inhibitors, all at physiological pH values. Kinetic analysis takes advantage of a sensitive and continuous assay for adenine linked to luciferase-based light production (*13*). Saporin-L1 catalyzes the depurination of adenines from A-10 (an RNA stem−loop 5′-CGCGAGAGCG-3′ mimic of the sarcin−ricin loop), linear and covalently closed circular constructs related to A-10, and mammalian 80S ribosomes, all at physiological pH (Figure 1).

The transition state (TS) mimic 9-deazaadenine-9-methylene-*N*-hydroxypyrrolidine (DADMeA) replacement for adenosine in the RIP recognition GAGA tetraloop motif inhibits saporin-L1

†This work was supported by Grant CA072444 from the National Institutes of Health.

*To whom correspondence should be addressed. E-mail: vern@aecom.yu.edu. Phone: (718) 430-2813. Fax: (718) 430-8565.

Published on Web 09/18/2009

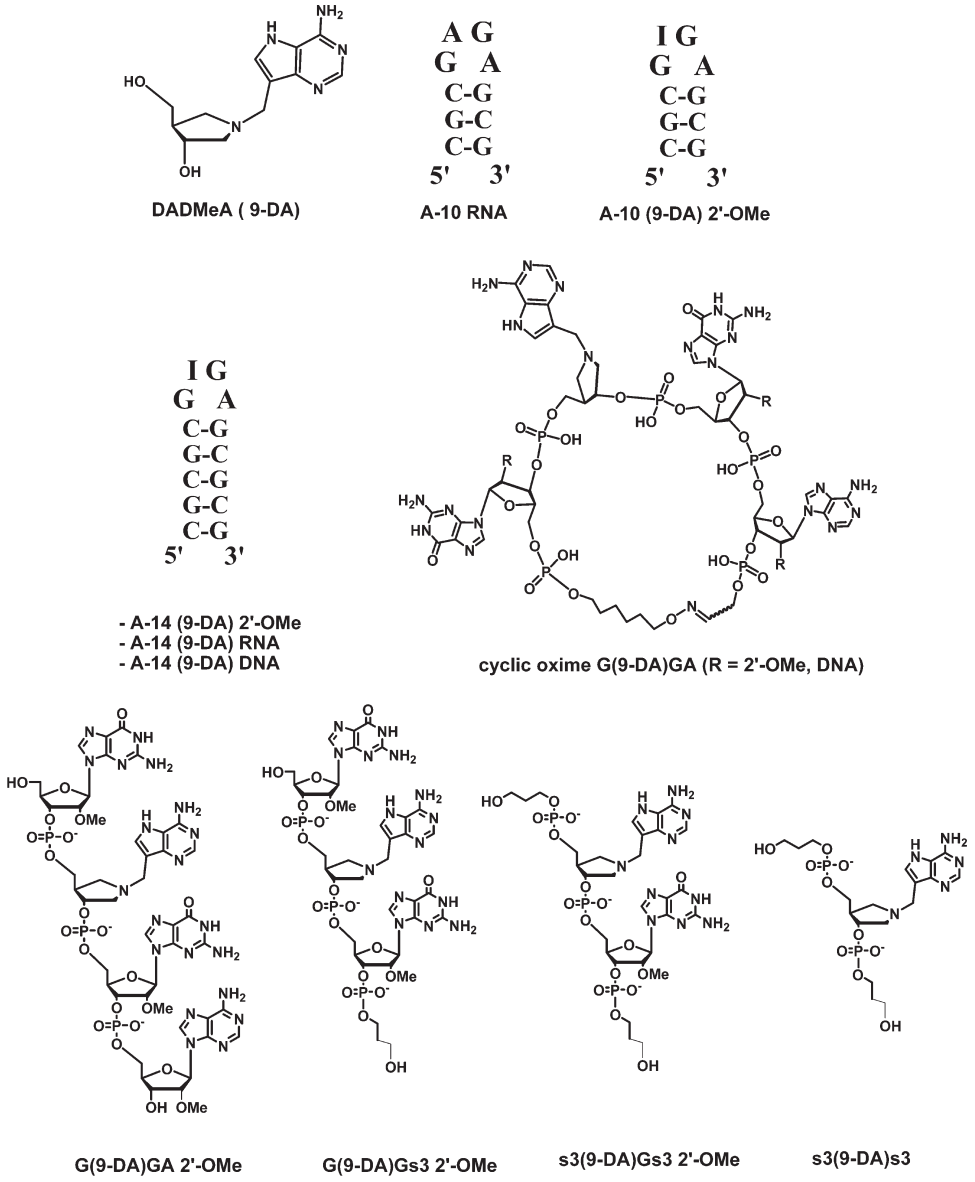

FIGURE 1: Substrate and inhibitor constructs for saporin-L1 assays and inhibition. The top row shows transition state mimic DADMeA (9-DA), a 9-deazaadenine *N*-hydroxypyrrolidine sugar. The A-10 RNA stem−loop substrate contains the GAGA tetraloop motif and alternating C-G base pairs for stem structure and loop folding. A-10 (9-DA) 2′-OMe contains DADMeA at the target RIP depurination site of the GAGA tetraloop and contains 2′-OMe-modified bases (excluding DADMeA). The middle row shows three 14-mer constructs containing DADMeA, including A-14 (9-DA) 2′-OMe, RNA, or DNA scaffolds. Cyclic oxime G(9-DA)GA 2′-OMe or DNA constructs are tetramers with 5′- to 3′-oligonucleotide ends closed by a synthetic linker (*16*). The bottom row shows linear inhibitors: tetramer G(9-DA)GA 2′-OMe, trimer G(9-DA)Gs3 2′-OMe, dimer s3(9-DA)Gs3 2′-OMe, and monomer s3(9-DA)s3, where s3 denotes a propanol phosphate.

catalysis (Figure 1). We synthesized inhibitors against saporin-L1, including monomer to 14-mer oligonucleotides, employing the DADMeA transition state mimic (Figure 1). Stem−loop inhibitor constructs, cyclic tetramer 5′ to 3′ covalently closed circular GAGA tetraloops, and monomeric inhibitors were also applied to saporin-L1. A minimal saporin-L1 inhibitor scaffold with 2′-OMe-containing compounds designed to give enhanced nuclease stability provided inhibition of saporin-L1 to low nanomolar K_i values and also protected ribosomes from saporin-L1 action in rabbit reticulocyte lysates (Figure 1).

EXPERIMENTAL PROCEDURES

Materials. Oligonucleotide A-10 was purchased from Dharmacon (Lafayette, CO). 5′-DMT-protected 9-DA aza sugar was synthesized and purified as previously described (*8*). DNA/RNA synthesis reagents were purchased from Glen Research (Sterling, VA) and ChemGene Co. (Ashland, MA). HPLC purifications were preformed on a Waters 626 pump with a 996 photodiode array detector with Millennium software. The firefly luciferase ATP assay kit (ATPlite) was purchased from Perkin-Elmer (Waltham, MA). Phosphatase inhibitors (PhosSTOP) were purchased from Roche Applied Science (Indianapolis, IN). RNase inhibitor (SuperRNasin) was purchased from Ambion (Austin, TX). Ricin A-chain and saporin-S6 was purchased from Aldrich Chemical Corp. (Ashland, MA). For translation assays, the Flexi Rabbit Reticulocyte Lysate System, the luciferase assay system, and rabbit reticulocyte lysate (untreated) was purchased from Promega (Madison, WI). Buffers and enzyme preparations were checked for RNase activity using RNaseAlert from Ambion. DEPC-treated water (0.1% DEPC stirred for 20 min followed by a 30 min autoclave treatment) was used in all enzymatic reactions and buffers. All other reagents used were

purchased at the highest available purity from Fisher Scientific (Pittsburgh, PA) or Aldrich Chemical Corp. Concentrations of adenine and oligonucleotides were measured using a NanoDrop 1000 instrument (Thermo Fisher Scientific, Waltham, MA). Inhibitor concentrations were determined spectrophotometrically, including the published millimolar extinction coefficient of 8.5 at 275 nm and pH 7 for 9-deazaadenosine (*14*). Enzyme concentrations of saporin-L1 and saporin-S6 were determined with the BCA protein assay kit from Pierce (Rockford, IL). Luminescence measurements were taken on a GloMax 96-well luminometer from Promega.

Saporin-L1 Isolation. Saporin-L1 was isolated from the leaves of *S. officinalis* (common soapwort) as described previously with modifications described below (*7*). Freshly harvested leaves (10 g) were frozen and ground with a pestle under liquid nitrogen. The powder was suspended in 80 mL of extraction buffer [10 mM Na_2HPO_4 (pH 5.5) (titrated with citric acid), 175 mM NaCl, 2.5 mM $MgCl_2$, 1 mM $CaCl_2$, one tablet of complet protease inhibitor (Roche), 1% (w/v) poly(vinylpolypyrrolidone), 1% cellulase, 0.5% hemicellulase, and 150 units of pectinase]. The mixture was stirred at room temperature for 3 h and then acidified to pH 4.0 with acetic acid. Triton X-100 was added to a final concentration of 0.5% (v/v), and the mixture was stirred for an additional 1 h. The digested and lysed leaf mixture was then filtered through cheese cloth and centrifuged at 25000*g* for 30 min. The supernatant was loaded on SP-Sepharose FF resin (Amersham) pre-equilibrated in 10 mM sodium phosphate (pH 4.5). The column was extensively washed with 10 mM sodium phosphate (pH 7.4), and the crude saporin-L1-containing fraction was eluted with the same buffer containing 1 M NaCl. The eluate was dialyzed against 10 mM sodium phosphate (pH 7.4), titrated to pH 4.5 with acetic acid, and loaded onto carboxymethyl-FF (three 1 mL columns, Amersham) pre-equilibrated in buffer [10 mM sodium phosphate (pH 7.4)]. The columns were washed extensively with buffer to achieve pH equilibration. Saporin-L1 was eluted with a 50 min linear gradient from 0 to 300 mM NaCl in 10 mM sodium phosphate (pH 7.4) at a rate of 1 mL/min and was identified as an ~30 kDa band by sodium dodecyl sulfate−polyacrylamide gel electrophoresis (SDS−PAGE). Saporin-L1 fractions were combined, titrated to pH 4.5 with acetic acid, and loaded onto heparin HP (three 1 mL columns, Amersham) pre-equilibrated in buffer. Saporin-L1 was eluted with a 50 min linear gradient from 0 to 800 mM NaCl in 10 mM sodium phosphate (pH 7.4) (1 mL/min). Saporin-L1 was eluted as the last major peak in the chromatogram and was identified by SDS−PAGE. The >80% pure saporin-L1 was concentrated with a spin Amicon concentrator and purified to >95% homogeneity with a BioSep-SEC-S 2000 column (Phenomenex) equilibrated in 20 mM sodium phosphate (pH 7.4) and eluted at a rate of 1 mL/min (Supporting Information). The gel filtration purification step was needed to remove trace DNAase and RNAase activities from saporin-L1. Saporin-L1 was concentrated to ~1 mg/mL and stored at 4 °C. The yield was ~0.5 mg of saporin-L1 from 10 g of leaf material. Isolation of saporin-L1 from *S. officinalis* seeds is described in the Supporting Information. Commercial saporin-S6 was purified with the heparin chromatography step as described above.

Saporin-L1 N-Terminal Sequencing and Mass Analysis. Purified saporin-L1 from the leaves of *S. officinalis* was verified by N-terminal sequencing at the Rockefeller University Proteomics Resource Center (New York, NY). The N-terminal sequence was VIIYELNLQG which matched previous reports for the saporin-L1 isoform (*7*). The mass of saporin-L1 was measured on a MALDI-TOF mass spectrometer in the linear positive ion mode with external calibration. Protein samples (~20 μM) were desalted with a ZipTip (Waters) as described by the manufacturer and eluted onto a 100-well gold plate with 1 μL of matrix solution (20 mg/mL sinapic acid in a 70% acetonitrile/H_2O with 0.1% TFA). The mass of saporin-L1 (28749 Da) isolated from the leaves of *S. officinalis* was comparable to previous reported masses for saporin-L1 leaf and vacuolar isoforms (28740−28765 Da) (Supporting Information) (*15*).

Synthesis of Oligonucleotide Inhibitors. Cyclic oligonucleotides and 1-aza sugar phosphoramidites were synthesized and purified as reported previously (*16*). Stem−loop oligonucleotides were synthesized on a 1 μmol scale with DMT-on mode using an Expedite 8909 DNA/RNA synthesizer following standard synthesis protocols for β-cyanoethyl phosphoramidite chemistry with acetyl-protected cytosine phosphoramidite and 5-benzylthio-1*H*-tetrazole as the activator. Cleavage from solid support and base deprotection of a 1 μmol synthesis was accomplished in 1.5 mL of AMA reagent (1:1 concentrated NH_4OH to 40% aqueous methylamine) for 45 min at 37 °C. The reaction mixture was centrifuged, the supernatant collected, and the resin washed twice with a 3:1:1 ethanol/acetonitrile/water mixture. Combined supernatant and washes were evaporated to dryness under vacuum. 2′-O-TBDMS deprotection of the A-14 (DADMeA) RNA (1 μmol) was accomplished using 250 μL of an anhydrous TEA HF/NMP solution (1.5 mL of *N*-methylpyrrolidinone, 750 μL of TEA, and 1.0 mL of TEA-3HF) heated to 65 °C for 2 h (*17*). This reaction mixture was diluted with 2 mL of 0.5 M NH_4OAc and evaporated to dryness under vacuum.

HPLC purification of the 5′-trityl stem−loop oligonucleotides was accomplished to >95% purity on a Waters Delta-Pak (7.9 mm × 300 mm) semipreparative C18 reversed phase column at a rate of 3.5 mL/min in a 20 mM NH_4OAc/5% CH_3CN mixture with a linear 0 to 40% gradient of CH_3CN over 25 min. Trityl-protected oligonucleotides were the major peak and eluted at ~25 min. The major late-eluting fraction was evaporated to dryness under vacuum. The pellet was dissolved in 1 mL of 80% acetic acid in water and incubated at 30 °C for 1 h, and the solution was evaporated to dryness under vacuum. HPLC purification of the final oligonucleotide was accomplished to >95% purity on a Waters Delta-Pak (7.9 mm × 300 mm) semipreparative C18 reversed phase column at a rate of 3.5 mL/min in 50 mM triethylammonium acetate (pH 7.0) with a linear 0 to 80% gradient of 50% aqueous methanol over 40 min. The final product was evaporated to dryness in a speed vac concentrator and resuspended in sterile RNAase-free water.

Linear inhibitors were synthesized in DMT-off mode on an Expedite 8909 synthesizer under conditions otherwise identical to those used for stem−loop oligonucleotides. After deprotection in AMA, the oligonucleotides were purified by HPLC to >95% purity as described for stem−loop structures in 50 mM triethylammonium acetate (pH 7.0) with a linear 0 to 50% gradient of 50% aqueous methanol over 40−60 min.

Stem−loop, cyclic, and linear oligonucleotide structures were confirmed using a MALDI-TOF mass spectrometer as described previously (*16*). Observed and calculated masses for the final compounds are given as Supporting Information. Prior to use in inhibition assays, stem−loop oligonucleotides were heated to 95 °C for 1 min and cooled on ice.

Saporin-L1 Kinetic Assay. The kinetics of saporin-L1 on substrate A-10 RNA (5′-CGCGAGAGCG-3′) were determined

using a continuous coupled assay for quantifying free adenine by linking it to the production of light from luciferase (*13*). In brief, 2× assay buffer was prepared in two steps: [50 mL of charcoal-filtered solution containing 100 mM tris-acetate (pH 7.7), 2 mM phosphoenolpyruvic acid, 2 mM sodium pyrophosphate, 2 mM 5-phospho-D-ribosyl-1-pyrophosphate (PRPP), 15 mM NH_4SO_4, 15 mM $(NH_4)_2MoO_4$, and phosphatase inhibitors in RNAase-free water] was stored at −80 °C in 1 mL aliquots. Prior to use, the assay buffer was completed by the addition of 10 mM $MgSO_4$, 8 units of APRTase, 8 units of phosphoenolpyruvate dikinase, 200 μL of D-luciferin/luciferase (ATPLite) reagent, and 1 μL of SuperRNasin (Ambion) per 1 mL of 2× assay buffer. One unit of enzyme activity was defined as the amount that forms 1 μmol of product/min at 20 °C.

Varying concentrations of A-10 RNA (5′-CGCGAGAGCG-3′) were mixed 1:1 with assay buffer in a 96-well luminometer plate, and reactions were initiated with 300 pM saporin-L1 (50 μL total reaction volume). Luminescence was measured with a luminometer in kinetic acquisition mode for several minutes. Adenine standards were prepared under identical assay conditions. The initial rates of adenine formation were calculated by converting the luminescence rate (lumens per second) to the enzymatic rate (picomoles of adenine per minute per picomole of enzyme) calibrated from the adenine standard curve. Kinetic parameters k_{cat} and K_m were calculated by fitting initial rates to the Michaelis−Menten equation, and inhibitor dissociation constants were obtained by fitting the data to the equation for competitive inhibition with the assumption that substrate and inhibitor act as competitive inhibitors.

Rabbit ribosomes (80S) were purified from the rabbit reticulocyte lysate by sucrose cushion centrifugation (*13*). Saporin-L1 (300 pM) was analyzed for kinetic parameters with ribosomes as the substrate as described for the A-10 RNA substrate. The ribosome concentration was determined by depurinating (to completion) two stock concentrations with 500 nM RTA and comparing the final luminescence to the adenine standard curve fit. RTA releases 1 mol of adenine from 1 mol of ribosome and thus provides a method of quantitation.

Saporin-L1 Inhibition Assays. Saporin-L1 inhibition constants for stem-loop, circular, and linear oligonucleotides were determined in a competition assay using RNA A-10 substrate with quantitative analysis of adenine release as described for kinetic assays. Varying concentrations of inhibitor were preincubated with 300 pM saporin-L1 for 10 min in 1× continuous assay buffer at 20 °C. Reactions were initiated by the addition of A-10 (~80 μM), and light generation (RLU) was assessed in a luminometer over several minutes to yield the initial rates (lumens per second). The maximum rate of catalysis (k_{cat}) was calculated from the Michaelis equation as described in kinetic assays. In cases where slow-onset inhibition was observed, K_i* was used to define the inhibition. Preincubation of inhibitor with saporin-L1 followed by initiation of the reaction with substrate provided a direct measure of K_i*. Values for the inhibition constant (K_i*) were calculated by fitting post slow-onset rates to the equation for competitive inhibition, $v = k_{cat}[S]/[[S] + K_m(1 + I/K_i^*)]$, where v is the initial reaction rate, [S] is the substrate concentration, K_m is the Michaelis constant for A-10, and k_{cat} is the initial rate at A-10 saturation. For tight inhibition, when the concentration of inhibitor was ≤5 times greater than the enzyme concentration, a correction was made for free inhibitor concentration. The free inhibitor concentration was determined by the relationship $I = I_t - (1 - v_i/v_o)E_t$, where I_t is total inhibitor concentration, v_i and v_o are the inhibited and uninhibited steady state rates, respectively, and E_t is the total enzyme concentration.

Protein Translation Assays. Saporin-L1 inhibition of protein translation was assessed using a reticulocyte lysate translation system to express luciferase from mRNA as described by the manufacturer. For the determination of IC_{50}, 30 μL translation reaction mixtures in triplicate with varying concentrations of saporin-L1 were incubated at 37 °C for 1.5 h. A 10 μL aliquot was sampled, and luminescence was measured with a luciferase detection kit (Promega) according to the manufacturer's protocol in a 96-well plate format on a luminometer. The percent translation relative to control was plotted versus the log of saporin-L1 concentration and fit to a dose−response curve for the calculation of IC_{50}.

For the determination of EC_{50}, triplicate reaction mixtures of 2.1 nM saporin-L1 with increasing inhibitor concentrations were preincubated at room temperature for 10 min in 5 μL of buffer [20 mM tris-acetate (pH 7.4), 25 mM KCl, and 5 mM $MgCl_2$]. Translation mix (25 μL) was added (final saporin-L1 concentration of 300 pM) to the preincubated samples, and they were incubated at 37 °C for 1.5 h. A 10 μL aliquot was sampled, and luminescence was measured with the luciferase detection kit (luminescence) as described above. A control with the maximum inhibitor concentration without saporin-L1 established that the oligonucleotide itself did not affect luciferase expression. The percent translation relative to control (no saporin-L1) was plotted versus the log of inhibitor concentration and was fit to a dose−response curve for the calculation of EC_{50}.

RESULTS AND DISCUSSION

Saporin-L1 Catalysis. Initial rate kinetics were measured by coupling the adenine product to a luciferase−luciferin coupled assay with quantitation via luminescence (*13*). Saporin-L1-catalyzed deadenylation of A-10 gave a hyperbolic saturation curve with a k_{cat} of 440 ± 16 min^{-1} and a K_m of 95 ± 7 μM at pH 7.7 (Table 1). MALDI-TOF analysis of the saporin-L1 reaction product showed that both adenosines in the GAGA tetraloop of A-10 were depurinated during prolonged incubations (Supporting Information). Cyclic oxime RNA GAGA, a circular oligonucleotide substrate, was also depurinated by saporin-L1 with kinetics comparable to those of A-10 RNA with a k_{cat} of 301 ± 27 min^{-1} and a K_m of 82 ± 15 μM (Table 1). The synthetic linker in circular oxime GAGA substrates folds the tetraloop for RIP recognition and is proposed to mimic the structure of stem−loop oligonucleotides (Figure 1) (*16*). Linear GAGA was also investigated as a saporin-L1 substrate and gave a k_{cat} of 293 ± 29 min^{-1} and a K_m of 266 ± 39 μM (Table 1). The K_m for linear GAGA is ~3-fold higher than for A-10 or cyclic oxime RNA substrate, while the catalytic turnover rate (k_{cat}) is comparable. Linear GAGA is less structured in solution than stem−loop or

Table 1: Kinetic Parameters for Saporin-L1

substrate	k_{cat} (min^{-1})	K_m (μM)	k_{cat}/K_m (M^{-1} s^{-1})
A-10 RNA	440 ± 16	95 ± 7	7.7×10^4
cyclic oxime GAGA	301 ± 27	82 ± 15	6.1×10^4
linear GAGA	293 ± 29	266 ± 39	1.8×10^4
poly(A)[a]	61 ± 1	639 ± 32	1.6×10^3
A-10 RNA (saporin-S6)	0.35 ± 0.04	360 ± 60	16

[a]Kinetic constants for poly(A) were previously reported in 20 mM Tris-HCl (pH 7.8), 100 mM NH_4Cl, and 10 mM magnesium acetate (*5*).

cyclic oligonucleotides and requires higher concentrations for equivalent catalytic rates. To the best of our knowledge, previous kinetic constants for saporin-L1 catalysis have only been reported for poly(A) RNA, with a k_{cat} of 61 ± 1 min^{-1} and a K_m of 639 ± 32 μM at pH 7.8 (Table 1) (*5*). A-10 RNA depurination by saporin-L1 is 10-fold faster (k_{cat}) and 4.5-fold tighter (K_m) than that of poly(A) RNA under comparable conditions, to give a 45-fold increased catalytic efficiency (k_{cat}/K_m).

Saporin-S6 Catalysis. Although saporin-S6 is more highly characterized than saporin-L1, it was resistant to inhibition by the transition state analogues. We measured A-10 catalysis by saporin-S6, an RIP from *S. officinalis* seeds. Saporin-S6 was a commercial preparation and was further purified to remove contaminating saporin-L1 (Experimental Procedures). Saporin-S6 and saporin-L1 coeluted on carboxymethyl resin but were separated by heparin chromatography (Supporting Information). Saporin-S6 initial rate catalysis with A-10 RNA as a substrate gave a k_{cat} of 0.35 ± 0.04 min^{-1} and a K_m of 360 ± 60 μM at pH 7.7 (Table 1). Saporin-L1 catalyzes (k_{cat}) A-10 RNA approximately 1500 times faster and has a 4-fold lower K_m than saporin-S6. Thus, saporin-L1 is 4800-fold more efficient (k_{cat}/K_m) at catalyzing A-10 RNA depurination than saporin-S6 (Table 1). Ricin A-chain is incapable of a single turnover of A-10 above pH 6.5 but at pH 4.0 gives a k_{cat} of ~4 min^{-1} on this substrate (*18*). Saporin-S6 was previously reported to catalyze the depurination of a 35-mer synthetic SRL mimic with a GAGA tetraloop at pH 7.6 with a k_{cat} of 0.4 min^{-1} and a K_m of 9 μM, while RIPs trichosanthin, gelonin, cinnamomin A-chain, and ricin A-chain had no detectable activity at physiological pH values (*19*).

Action of Saporin-L1 on 80S Ribosomes. Action of saporin-L1 on 80S rabbit reticulocyte ribosomes (40 nM) showed multiple adenines released with a rate of 50 min^{-1} which is 250-fold faster than the rate of release of adenine from A-10 RNA at an equivalent concentration. We observed a continuous, linear rate for the formation of adenine from 80S rabbit ribosomes extending beyond one adenine per ribosome. Thus, saporin-L1 lacks sarcin−ricin loop specificity as the primary ribosomal depurination target. Previous reports indicate that saporin-L1 depurinates up to 36 adenines/mol from 80S rat ribosomes while saporin-S6 releases 1−2.5 adenines/mol (*20*). Moreover, saporin-L1 was reported to release ~6 adenines from the 80S rat ribosome before 50% inhibition of protein synthesis was observed in in vitro translation assays with a poly(U) transcript (*5*). Thus, adenines other than those at the sarcin−ricin loop are removed preferentially. Most other ribosome inactivating proteins are highly specific in releasing 1 mol of adenine/mol of ribosome from the eukaryotic sarcin−ricin loop (*1*). Thus, both ricin A-chain and saporin-S6 release only 1 mol of adenine/mol of 80S rabbit ribosome under our assay conditions. Ribosomal proteins surrounding the sarcin−ricin loop are known to influence the ribotoxic mechanism of RIP substrate recognition (*21*, *22*).

Saporin-L1 Inhibitors. DADMeA (9-DA in the figures) is a nonhydrolyzable methylene-bridged 9-deazaadenine 1-aza sugar with features of the transition state for depurination of A-10 constructs by ricin A-chain. The replacement of N for C at C1′ of the ribosyl group mimics the carbocation of the dissociated transition state (*8*, *10*). Replacing adenine with 9-deazaadenine caused an elevated pK_a at N7, another feature of the transition state. The methylene linker between the 9-deazaadenine and the hydroxypyrrolidine places the base analogue and ribocation at approximately the same distance as found at the transition state. The omission of the 2′-hydroxyl found in RNA is required for the chemical stability of 9-DA. Replacing the scissile adenosine with 9-DA within the 14-mer stem−loop structure [A-14 (9-DA) RNA] resulted in an inhibitor (A-10 RNA as a substrate) with a K_i* of 3.7 ± 0.7 nM at pH 7.7 (Table 2). The slow-onset inhibition (K_i*) observed for saporin-L1 binding of inhibitors such as A-14 (9-DA) RNA was common to all inhibitor constructs listed in Table 1 excluding s3(9-DA)s3 and 9-DA (Figure 2). Inhibitor A-14 (9-DA) DNA oligonucleotide inhibited saporin-L1 with a K_i* of 3.1 ± 0.5 nM, similar to that of A-14 (9-DA) RNA (Table 2). 2′-OMe A-14 (9-DA), a nuclease stable 14-mer oligonucleotide, is also similar to the RNA/DNA versions with a K_i* value of 5.6 ± 0.8 nM (Table 2). Thus, high binding affinity is observed for A-14 (9-DA) constructs in RNA, DNA, and 2′-OMe structural motifs. A 10-mer inhibitor A-10 (9-DA)

Table 2: Inhibition Constants for Saporin-L1 Inhibitors[a]

inhibitor	K_i* (nM)	inhibitor	K_i* (nM)
A-14 (9-DA) 2′-OMe	5.6 ± 0.8	G(9-DA)GA 2′-OMe	8.7 ± 2.3
A-14 (9-DA) RNA	3.7 ± 0.7	G(9-DA)Gs3 2′-OMe	7.5 ± 1.6
A-14 (9-DA) DNA	3.1 ± 0.5	s3(9-DA)Gs3 2′-OMe	6.4 ± 1.7
A-10 (9-DA) 2′-OMe	4.2 ± 1.3	s3(9-DA)s3	690 ± 100[b]
cyclic oxime (9-DA) 2′-OMe	3.9 ± 0.5	9-DA	> 0.5 × 10^{6}[b]
cyclic oxime (9-DA) DNA	2.3 ± 0.1		

[a]See Figure 1 for structures of inhibitors. [b]K_i values with no slow onset observed.

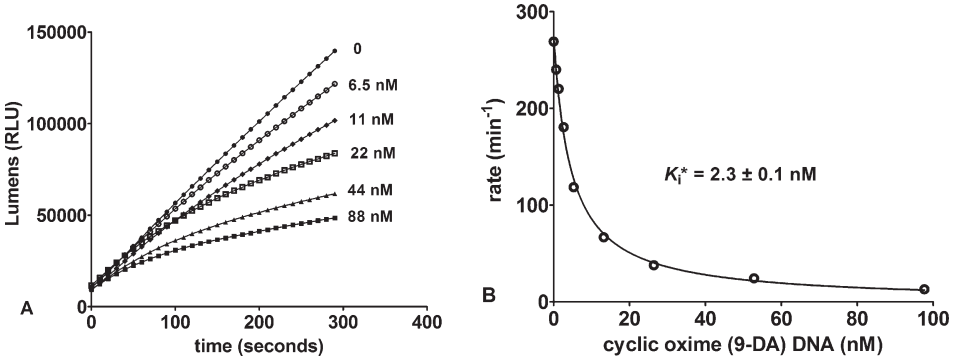

FIGURE 2: Slow-onset inhibition of saporin-L1 by transition state mimics. (A) Plot of lumens (RLU) vs time for saporin-L1 catalysis of A-10 with increasing inhibitor [A14 (9-DA) 2′-OMe] concentrations. (B) Competitive inhibition curve fit of rate vs increasing concentrations of tetramer cyclic oxime G(9-DA)GA DNA inhibitor. Kinetics were measured after a 10 min enzyme−inhibitor preincubation equilibration to achieve slow-onset binding (K_i*).

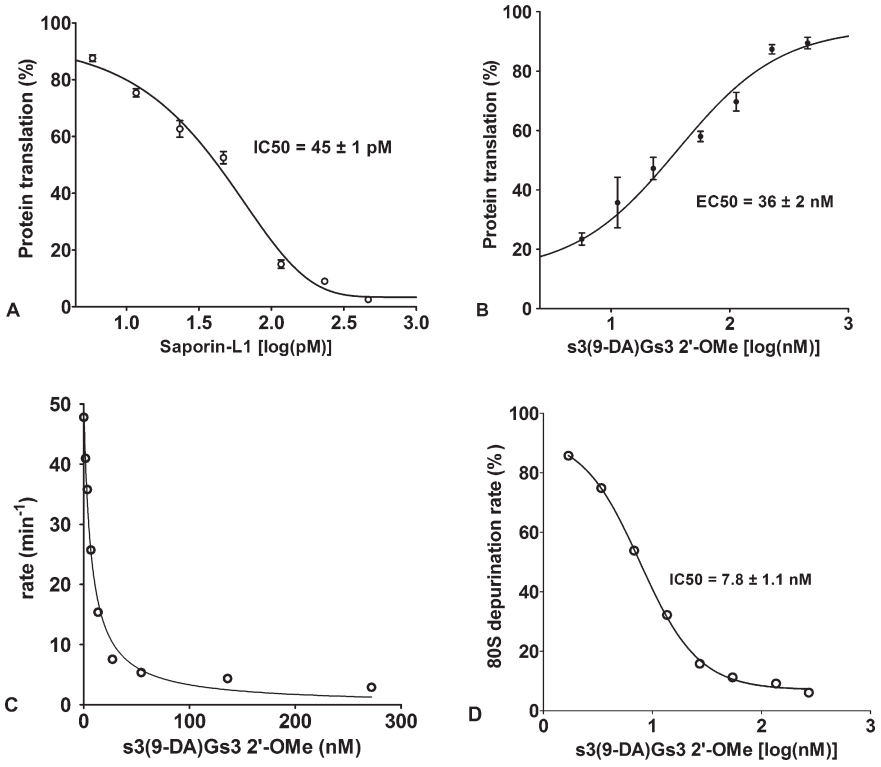

FIGURE 3: Inhibition of translation by saporin-L1 and protection by saporin-L-1 inhibitors. (A) Saporin-L1 inhibition of protein translation (percent relative to control) in rabbit reticulocyte lysate assays. The mean and standard error of the mean (SEM) of triplicate data points were fit to a dose−response curve. (B) Protein translation rescue from 300 pM saporin-L1 (percent relative to no saporin-L1) with increasing concentrations [log(nanomolar)] of dimer s3(9-DA)Gs3 inhibitor in a ribosome reticulocyte lysate assay. The mean and SEM error of triplicate data points were fit to a dose−response curve. (C) Saporin-L1 (300 pM) rate of release of adenine from 40 nM 80S ribosome vs s3(9-DA)Gs3 inhibitor concentration. (D) Plot of panel C as a dose−response curve fit for the percentage of 80S catalysis [percent relative to no s3(9-DA)Gs3)] vs increasing concentrations [log(nanomolar)] of dimer s3(9-DA)Gs3 inhibitor. The zero inhibitor value shown in panel C is not plotted in panel D.

2′-OMe had a K_i* of 4.2 ± 1.3 nM, similar to that of 2′-OMe A-14 (9-DA) (Table 2). This observation is reminiscent of previous reports with ricin A-chain showing similar K_m values for small constructs of RNA, DNA, and 2′-OMe-modified substrates (*23*). Limited quantitative kinetic and substrate specificity data are available for other RIPs.

Circular Inhibitors. Cyclic DNA and cyclic 2′-OMe-modified G(9-DA)GA oligonucleotides inhibited saporin-L1 with K_i* values of 2.3 ± 0.1 and 3.9 ± 0.5 nM, respectively (Table 2 and Figure 2B). Thus, 9-DA cyclic tetramers inhibit saporin-L1 1.4-fold tighter than the larger A-14 stem−loop counterparts. This similarity in K_i* supports a primary role for the stem in sarcin−ricin stem−loop mimics in folding the tetraloop for RIP recognition (*16*). Circular oxime (9-DA) DNA binds saporin-L1 40000-fold tighter than A-10 RNA or cyclic oxime RNA substrate, an increase in binding energy of ∼6 kcal/mol.

Linear Inhibitors. We also investigated monomer, linear dimer, trimer, and tetramer inhibitor scaffolds containing 9-DA in the RTA scissile adenosine position (Figure 1). Linear tetramer G(9-DA)GA 2′-OMe bound saporin-L1 only ∼2-fold less tightly than its cyclic oxime counterpart and gave a K_i* of 8.7 ± 2.3 nM (Table 2). Linear trimer [G(9-DA)Gs3] and dimer [s3(9-DA)Gs3] 2′-OMe inhibitors bound comparably with K_i* values of 7.5 ± 1.6 and 6.4 ± 1.7 nM, respectively (Table 1 and Figure 1). The linear dimer s3(9-DA)Gs3 phosphodiester also binds with an affinity similar to those of stem−loop and cyclic oxime 2′-OMe inhibitors (Table 2). A monomer phosphodiester [s3(9-DA)s3] inhibited saporin-L1 with a K_i* value of 690 ± 100 nM, while 9-DA alone was not an inhibitor (Table 2). Dimer [s3(9-DA)Gs3] is the tightest linear inhibitor for saporin-L1, binding ∼15000-fold tighter than A-10 RNA, an increase in binding energy of ∼5.6 kcal/mol. Removal of the 3′-Gs3 moiety of the dimer inhibitor to give the monomer [s3(9-DA)s3] reduced the binding affinity for saporin-L1 10-fold and therefore the binding energy by ∼2-fold (Table 2). Thus, the 3′-Gs3 moiety of dimer s3(9-DA)Gs3 contributes half the binding energy for inhibitor association with saporin-L1. NMR structural determinations of GAGA tetraloops and the reported crystal structure of a 29-mer RNA SRL mimic show the $G_1A_2G_3A_4$ tretraloop conformation with A_2 and G_3 available for direct hydrogen bonding, while G_1 and A_4 form a sheared base pair (*24*, *25*). Surprisingly, none of the inhibitors for saporin-L1 (Table 2) were effective against saporin-S6 at concentrations up to 10 μM. Saporin-S6 also catalyzes A-10 deadenylation but at a much slower rate and with a higher K_m (Table 1).

Saporin-L1 Translation Inhibition. Saporin-L1 inhibited the translation of luciferase mRNA by rabbit reticulocyte lysate in a cell-free translation assay with an IC_{50} of 45 pM (Figure 3A). Previous reports of saporin-L1 inhibition (IC_{50}) in ribosome translational assays are comparable and vary from 250 pM to 11 nM with poly(U) mRNA for polyphenylalanine expression (*5*−*7*). Saporin-L1 has been reported to release more than 6 mol of adenine/ribosome to cause the arrest of translation (*5*). Although the sarcin−ricin loop is not the first adenylate targeted by saporin-L1 in the 80S ribosome, the robust depurination activity is highly toxic to ribosomes and protein translation. Ricin A-chain and saporin-S6 specifically depurinate the sarcin−ricin loop and have IC_{50} values of 30 and 8 pM, respectively, in rabbit reticulocyte lysate translation assays, similar to that of 45 pM for saporin-L1 (Figure 3A) (*26*).

Saporin-L1 Inhibitor Implications for Toxin Immunotherapy. Saporin-L1 immunotoxin conjugates have been shown to be as cytotoxic to cells as saporin-S6 conjugates (*27*). The catalytic A-chains of saporin-S6 and ricin have been investigated as anticancer agents in phase I/II clinical trials using chimeric immunotoxin conjugates in the treatment of lymphomas (*11*, *28*−*30*). Therapeutic uses of immunotoxins have been limited by the vascular leak syndrome, a side effect resulting from inappropriate toxin targeting to the capillary bed of endothelial cells, causing edema and multiorgan failure (*12*, *31*−*33*). Thus, cancer therapies that employ RIP-linked immunotoxins remain a challenge. Inhibitors to RIPs could provide a way to rescue normal cells following treatment of a targeted tissue with immunotoxins.

Saporin-L1 Translation Inhibition Rescue by the TS Inhibitor. Protein translation, its inhibition by saporin-L1, and its rescue by inhibitors were studied in rabbit reticulocyte preparations. The minimal saporin-L1 inhibitor dinucleotide s3(9-DA)Gs3 2′-OMe was used (Figure 1). The toxicity of saporin-L1 to cell-free translation caused ~90% inhibition at 300 pM saporin-L1 and was rescued by increasing concentrations of s3(9-DA)Gs3 with an EC_{50} of 36 ± 2 nM (Figure 3B). The EC_{50}:K_i* ratio for s3(9-DA)Gs3 comparing translation assays and inhibition kinetics was ~6, supporting strong saporin-L1 inhibition in complex assays at physiological pH (Figure 3B and Table 2). Dinucleotide s3(9-DA)Gs3 also inhibits saporin-L1 release of adenine from purified 80S rabbit ribosomes and gave an IC_{50} of 7.8 ± 1.1 nM (Figure 2C,D). The calculation of a K_m value for 80S rabbit ribosomes was limited by practical concentrations of ribosomes from reticulocyte lysate and therefore precluded direct K_i* calculation. However, the IC_{50} value for s3(9-DA)Gs3 was comparable to the K_i* measured for s3(9-DA)Gs3 in A-10 competition assays (Figure 2D and Table 2). Thus, TS inhibitors of saporin-L1 are equally effective in preventing ribosome depurination and depurination of small nucleic acid substrates.

SUMMARY AND CONCLUSIONS

Saporin-L1 is highly active on mammalian ribosomes and potently inhibited by the transition state mimic DADMeA (9-DA) when incorporated into the depurination site of stem−loop, circular, and linear nucleic acid scaffolds appropriate for RIP recognition. This activity occurs under physiological conditions. The oligonucleotide context is essential as 9-DA alone is a poor inhibitor. Small oligonucleotide inhibitors featuring DADMeA bind up to 40000-fold tighter than small stem−loop RNA substrates. Nine inhibitors exhibited slow-onset binding to saporin-L1 with dissociation constants from 8.7 to 2.3 nM. Inhibitors constructed on RNA, 2′-OMe, and DNA scaffolds supported 9-DA binding with only small scaffold effects. Covalently closed circular inhibitors constructed on DNA or 2′-OMe RNA scaffolds were also excellent inhibitors. Dinucleotide s3(9-DA)Gs3 was the smallest tight-binding inhibitor of saporin-L1. In ribosome translation rescue assays, s3(9-DA)Gs3 restored protein synthesis by inhibiting saporin-L1 depurination activity. Direct competition assays between 80S rabbit ribosomes and s3(9-DA)Gs3 established saporin-L1 inhibition with a dissociation constant of 7.8 nM.

Transition state inhibitor efficacy for RIP activity at physiological pH has been previously limited by the pH 4.0 activity used for the development of ricin A-chain transition state analogues. Ricin A-chain and other type I and II RIPs have a low pH catalytic optimum on nucleic acid substrates such as stem−loop RNA, poly(A), and/or hsDNA, while the natural ribosome substrate is depurinated optimally at physiological pH (*6*, *18*, *34*). Saporin-S6 has a substrate specificity distinct from that of saporin-L1 and was not inhibited by saporin-L1 transition state mimics at neutral pH. Saporin-L1 rapidly catalyzes depurination of stem−loop, circular, and linear truncated mimics of the sarcin−ricin loop at neutral pH, a unique feature in the RIP family of *N*-glycohydrolases (Table 1) (*35*). Although saporin-L1 is reported to catalyze release of adenine from poly(A), hsDNA, tRNA, *E. coli* rRNA, and globin mRNA at pH 7.8 (*5*, *6*), the 80S ribosome is a preferred substrate.

Tight-binding inhibitors of saporin-L1 that prevent ribosome damage at physiological pH provide a breakthrough in the development of immunotoxin cancer therapy. It should be possible to use saporin-L1 conjugates to target cancer cells. Following tumor lysis, rescue of the organism from vascular leak syndrome might be effected with the small, stable, and tight-binding inhibitors of saporin-L1 characterized here.

SUPPORTING INFORMATION AVAILABLE

Details of saporin-L1 purification, mass spectral characteristics of chemically synthesized oligonucleotides, and curve fits of kinetic data to yield the kinetic and inhibition constants for saporin-L1. This material is available free of charge via the Internet at http://pubs.acs.org.

REFERENCES

1. Endo, Y., Mitsui, K., Motizuki, M., and Tsurugi, K. (1987) The mechanism of action of ricin and related toxic lectins on eukaryotic ribosomes. The site and the characteristics of the modification in 28 S ribosomal RNA caused by the toxins. *J. Biol. Chem. 262*, 5908–5912.
2. Polito, L., Bortolotti, M., Farini, V., Battelli, M. G., Barbieri, L., and Bolognesi, A. (2009) Saporin induces multiple death pathways in lymphoma cells with different intensity and timing as compared to ricin. *Int. J. Biochem. Cell Biol. 41*, 1055–1061.
3. Barbieri, L., Valbonesi, P., Bonora, E., Gorini, P., Bolognesi, A., and Stirpe, F. (1997) Polynucleotide:adenosine glycosidase activity of ribosome-inactivating proteins: effect on DNA, RNA and poly(A). *Nucleic Acids Res. 25*, 518–522.
4. Barbieri, L., Valbonesi, P., Govoni, M., Pession, A., and Stirpe, F. (2000) Polynucleotide:adenosine glycosidase activity of saporin-L1: Effects on various forms of mammalian DNA. *Biochim. Biophys. Acta 1480*, 258–266.
5. Barbieri, L., Valbonesi, P., Gorini, P., Pession, A., and Stirpe, F. (1996) Polynucleotide:adenosine glycosidase activity of saporin-L1: Effect on DNA, RNA and poly(A). *Biochem. J. 319*, 507–513.
6. Barbieri, L., Ciani, M., Girbés, T., Liu, W., VanDamme, E. J. M., Peumans, W. J., and Stirpe, F. (2004) Enzymatic activity of toxic and non-toxic type 2 ribosome-inactivating proteins. *FEBS Lett. 563*, 219–222.
7. Ferreras, J. M., Barbieri, L., Girbés, T., Battelli, M. G., Rojo, M. A., Arias, F. J., Rocher, M. A., Soriano, F., Mendéz, E., and Stirpe, F. (1993) Distribution and properties of major ribosome-inactivating proteins (28 S rRNA N-glycosidases) of the plant *Saponaria officinalis* L. (Caryophyllaceae). *Biochim. Biophys. Acta 1216*, 31–42.
8. Roday, S., Amukele, T., Evans, G. B., Tyler, P. C., Furneaux, R. H., and Schramm, V. L. (2004) Inhibition of Ricin A-Chain with Pyrrolidine Mimics of the Oxacarbenium Ion Transition State. *Biochemistry 43*, 4923–4933.
9. Chen, X.-Y., Berti, P. J., and Schramm, V. L. (2000) Transition-State Analysis for Depurination of DNA by Ricin A-Chain. *J. Am. Chem. Soc. 122*, 6527–6534.
10. Chen, X.-Y., Berti, P. J., and Schramm, V. L. (2000) Ricin A-Chain: Kinetic Isotope Effects and Transition State Structure with Stem-Loop RNA. *J. Am. Chem. Soc. 122*, 1609–1617.
11. Schnell, R., Borchmann, P., Staak, J. O., Schindler, J., Ghetie, V., Vitetta, E. S., and Engert, A. (2003) Clinical evaluation of ricin

A-chain immunotoxins in patients with Hodgkin's lymphoma. *Ann. Oncol. 14*, 729–736.
12. Baluna, R., and Vitetta, E. S. (1997) Vascular leak syndrome: A side effect of immunotherapy. *Immunopharmacology 37*, 117–132.
13. Sturm, M. B., and Schramm, V. L. (2009) Detecting ricin: Sensitive luminescent assay for ricin A-chain ribosome depurination kinetics. *Anal. Chem. 81*, 2847–2853.
14. Singh, V., Evans, G. B., Lenz, D. H., Mason, J. M., Clinch, K., Mee, S., Painter, G. F., Tyler, P. C., Furneaux, R. H., Lee, J. E., Howell, P. L., and Schramm, V. L. (2005) Femtomolar transition state analogue inhibitors of 5′-methylthioadenosine/S-adenosylhomocysteine nucleosidase from *Escherichia coli*. *J. Biol. Chem. 280*, 18265–18273.
15. Angelis, F. D., Tullio, A. D., Spanò, L., and Tucci, A. (2001) Mass spectrometric study of different isoforms of the plant toxin saporin. *J. Mass Spectrom. 36*, 1237–1239.
16. Sturm, M. B., Roday, S., and Schramm, V. L. (2007) Circular DNA and DNA/RNA Hybrid Molecules as Scaffolds for Ricin Inhibitor Design. *J. Am. Chem. Soc. 129*, 5544–5550.
17. Wincott, F., DiRenzo, A., Shaffer, C., Grimm, S., Tracz, D., Workman, C., Sweedler, D., Gonzalez, C., Scaringe, S., and Usman, N. (1995) Synthesis, deprotection, analysis and purification of RNA and ribozymes. *Nucleic Acids Res. 23*, 2677–2684.
18. Chen, X. Y., Link, T. M., and Schramm, V. L. (1998) Ricin A-Chain: Kinetics, Mechanism, and RNA Stem-Loop Inhibitors. *Biochemistry 37*, 11605–11613.
19. Tang, S., Hu, R., Liu, W., and Ruan, K. (2000) Non-Specific Depurination Activity of Saporin-S6, a Ribosome-Inactivating Protein, under Acidic Conditions. *Biol. Chem. 381*, 769–772.
20. Barbieri, L., Ferreras, J. M., Barraco, A., Ricci, P., and Stirpe, F. (1992) Some ribosome-inactivating proteins depurinate ribosomal RNA at multiple sites. *Biochem. J. 286*, 1–4.
21. Vater, C. A., Bartle, L. M., Leszyk, J. D., Lambert, J. M., and Goldmacher, V. S. (1995) Ricin A chain can be chemically cross-linked to the mammalian ribosomal proteins L9 and L10e. *J. Biol. Chem. 270*, 12933–12940.
22. Chan, D. S., Chu, L. O., Lee, K. M., Too, P. H., Ma, K. W., Sze, K. H., Zhu, G., Shaw, P. C., and Wong, K. B. (2007) Interaction between trichosanthin, a ribosome-inactivating protein, and the ribosomal stalk protein P2 by chemical shift perturbation and mutagenesis analyses. *Nucleic Acids Res. 35*, 1660–1672.
23. Amukele, T. K., and Schramm, V. L. (2004) Ricin A-chain substrate specificity in RNA, DNA, and hybrid stem-loop structures. *Biochemistry 43*, 4913–4922.
24. Correll, C. C., Munishkin, A., Chan, Y. L., Ren, Z., Wool, I. G., and Steitz, T. A. (1998) Crystal structure of the ribosomal RNA domain essential for binding elongation factors. *Proc. Natl. Acad. Sci. U.S.A. 95*, 13436–13441.
25. Jucker, F. M., Heus, H. A., Yip, P. F., Moors, E. H., and Pardi, A. (1996) A network of heterogeneous hydrogen bonds in GNRA tetraloops. *J. Mol. Biol. 264*, 968–980.
26. Hale, M. (2001) Microtiter-Based Assay for Evaluating the Biological Activity of Ribosome-Inactivating Proteins. *Pharmacol. Toxicol. 88*, 255–260.
27. Barbieri, L., Bolognesi, A., Valbonesi, P., Polito, L., Olivieri, F., and Stirpe, F. (2000) Polynucleotide:Adenosine Glycosidase Activity of Immunotoxins Containing Ribosome-Inactivating Proteins. *J. Drug Targeting 8*, 281–288.
28. Blakey, D. C., Skilleter, D. N., Price, R. J., Watson, G. J., Hart, L. I., Newell, D. R., and Thorpe, P. E. (1988) Comparison of the Pharmacokinetics and Hepatotoxic Effects of Saporin and Ricin A-Chain Immunotoxins on Murine Liver Parenchymal Cells. *Cancer Res. 48*, 7072–7078.
29. Falini, B., Bolognesi, A., Flenghi, L., Tazzari, P., Broe, M., Stein, H., Dtirkop, H., Aversa, F., Corneli, R., Pizzolo, G., Barbabietola, G., Sabattini, E., Pileri, S., Martelli, M., and Stirpe, F. (1992) Response of refractory Hodgkin's disease to monoclonal anti-CD30 immunotoxin. *Lancet 339*, 1195–1196.
30. Polito, L., Bolognesi, A., Tazzari, P. L., Farini, V., Lubelli, C., Zinzani, P. L., Ricci, F., and Stirpe, F. (2004) The conjugate Rituximab/saporin-S6 completely inhibits clonogenic growth of CD20-expressing cells and produces a synergistic toxic effect with Fludarabine. *Leukemia 18*, 1215–1222.
31. Baluna, R., Rizo, J., Gordon, B. E., Ghetie, V., and Vitetta, E. S. (1999) Evidence for a structural motif in toxins and interleukin-2 that may be responsible for binding to endothelial cells and initiating vascular leak syndrome. *Proc. Natl. Acad. Sci. U.S.A. 96*, 3957–3962.
32. Baluna, R., Coleman, E., Jones, C., Ghetia, V., and Vitetta, E. S. (2000) The Effect of a Monoclonal Antibody Coupled to Ricin A Chain-Derived Peptides on Endothelial Cells in Vitro: Insights into Toxin-Mediated Vascular Damage. *Exp. Cell Res. 258*, 417–424.
33. Smallshaw, J. E., Ghetie, V., Rizo, J., Fulmer, J. R., Trahan, L. L., Ghetie, M. A., and Vitetta, E. S. (2003) Genetic engineering of an immunotoxin to eliminate pulmonary vascular leak in mice. *Nat. Biotechnol. 27*, 387–391.
34. Barbieri, L., Valbonesi, P., Bonora, E., Gorini, P., Bolognesi, A., and Stirpe, F. (1997) Polynucleotide:adenosine glycosidase activity of ribosome-inactivating proteins: Effect on DNA, RNA and poly(A). *Nucleic Acids Res. 25*, 518–522.
35. Barbieri, L., Gorini, P., Valbonesi, P., Castiglioni, P., and Stirpe, F. (1994) Unexpected activity of saporins. *Nature 372*, 624.